

# Functional Magnetic Resonance Imaging of Macaque Monkeys Performing Visually Guided Saccade Tasks: Comparison of Cortical Eye Fields with Humans

Minoru Koyama,<sup>1,3</sup> Isao Hasegawa,<sup>1,3</sup>  
Takahiro Osada,<sup>1,2</sup> Yusuke Adachi,<sup>1,2</sup>  
Kiyoshi Nakahara,<sup>1</sup> and Yasushi Miyashita<sup>1,2,\*</sup>

<sup>1</sup>Department of Physiology  
The University of Tokyo School of Medicine  
<sup>2</sup>Department of Physics  
The University of Tokyo School of Science  
7-3-1 Hongo, Bunkyo-ku  
Tokyo 113-0033  
Japan

## Summary

The frontal and parietal eye fields serve as functional landmarks of the primate brain, although their correspondences between humans and macaque monkeys remain unclear. We conducted fMRI at 4.7 T in monkeys performing visually-guided saccade tasks and compared brain activations with those in humans using identical paradigms. Among multiple parietal activations, the dorsal lateral intraparietal area in monkeys and an area in the posterior superior parietal lobule in humans exhibited the highest selectivity to saccade directions. In the frontal cortex, the selectivity was highest at the junction of the precentral and superior frontal sulci in humans and in the frontal eye field (FEF) in monkeys. BOLD activation peaks were also found in premotor areas (BA6) in monkeys, which suggests that the apparent discrepancy in location between putative human FEF (BA6, suggested by imaging studies) and monkey FEF (BA8, identified by microstimulation studies) partly arose from methodological differences.

## Introduction

Exploration of the visual environment is achieved in discrete steps wherein a rapid eye movement called saccade sequentially brings an object in the visual scene onto the fovea (the highest-acuity retinal region). A number of brain regions have been implicated in the control of saccadic eye movements in macaque monkeys (Andersen et al., 1997; Schall, 1997; Colby and Goldberg, 1999; Tehovnik et al., 2000) and humans (Corbetta et al., 1998; Luna et al., 1998; Petit and Haxby, 1999). However, despite great efforts that have been made for interspecies comparisons (Courtney et al., 1998; Bremner et al., 2001; Sereno et al., 2001; Tootell and Hadjikhani, 2001; Van Essen et al., 2001; Astafiev et al., 2003), it has been difficult to directly determine correspondences of the cortical oculomotor centers between humans and monkeys due to methodological differences.

The frontal eye field (FEF), a major brain center responsible for control of the saccadic eye movement, is a landmark structure demarcating anatomically and functionally distinct divisions of the frontal cortex

(Petrides and Pandya, 1994; Schall, 1997; Tehovnik et al., 2000). The human FEF has been assigned to Brodmann's cytoarchitectonic area 6 (BA 6) (Brodmann, 1909) by recent neuroimaging studies (Paus, 1996; Corbetta et al., 1998; Luna et al., 1998), whereas the monkey FEF has been assigned to BA 8 (Brodmann, 1905) by electrophysiological and microstimulation studies (Bruce and Goldberg, 1985; Bruce et al., 1985; Schall, 1997). In the posterior parietal cortex, oculomotor functions have been implicated in multiple areas in the superior parietal lobule in humans (Corbetta et al., 1998; Sereno et al., 2001) and lateral intraparietal areas in macaques (Andersen et al., 1997; Colby and Goldberg, 1999), but functional correspondences among them also remain elusive. These diversities emphasize the importance of direct comparison of the functional architecture of the frontal and parietal eye fields between humans and macaques by using common technologies and behavioral paradigms.

Recently, functional magnetic resonance imaging (fMRI) using macaque monkeys has been developed in both anesthetized (Dubowitz et al., 1998; Stefanacci et al., 1998; Hayashi et al., 1999; Logothetis et al., 1999, 2001) and awake (Vanduffel et al., 2001, 2002; Nakahara et al., 2002; Tsao et al., 2003a, 2003b) preparations. These studies have enriched our knowledge of the primate cortical organization, especially in striate and extrastriate visual areas, but our understanding of interspecies correspondences of the neocortical association areas is still fragmentary. In the present study, we used high-field fMRI at 4.7 T to obtain blood oxygenation level-dependent (BOLD) signals (Ogawa et al., 1990; Kwong et al., 1992) from monkeys performing saccadic eye movement tasks. We also conducted fMRI in humans (1.5 T) performing the same task as in the monkey experiments. Our primary objective was to provide direct evidence for the correspondences of functional architecture of the cortical eye fields between macaque monkeys and humans, with the use of a common methodology (BOLD fMRI) and identical behavioral paradigms. Especially, we intended to examine whether the apparent discrepancy of anatomical assignment of the human FEF (BA 6 by neuroimaging studies) and the monkey FEF (BA 8 by microstimulation and single-unit recording studies) could be ascribed to methodological differences or intrinsic species differences.

## Results

### Monkey fMRI Studies

Three awake macaque monkeys underwent functional scanning in a 4.7 T MRI scanner while they performed oculomotor tasks with their eye positions monitored by an infrared-sensitive CCD camera. We used blocked-design fMRI to identify brain regions activated during visually guided saccades compared to fixation baseline and also used event-related fMRI to examine the modulation of neural activity by saccade directions in regions of interest (ROIs) localized by the blocked-design fMRI results.

\*Correspondence: yasushi\_miyashita@m.u-tokyo.ac.jp

<sup>3</sup>These authors contributed equally to this work.

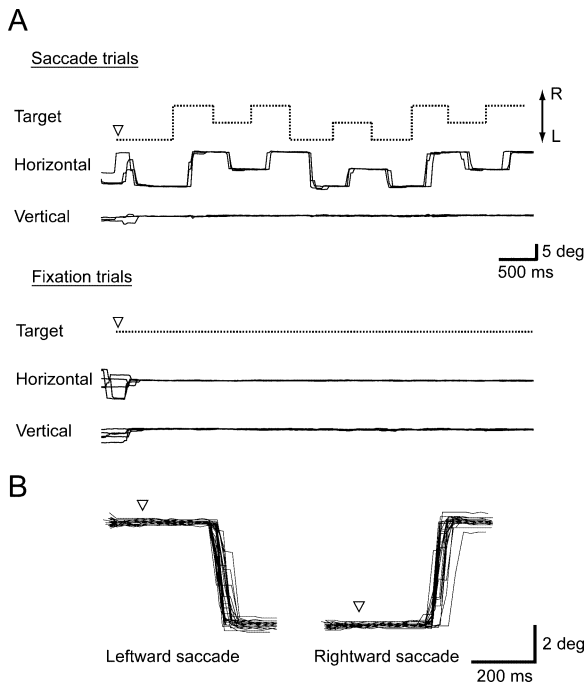


**Figure 1.** Oculomotor Tasks and Eye Movements of the Monkeys (A) Horizontal and vertical eye positions during the serial saccade trials (upper) and the fixation trials (lower). Dotted lines indicate the horizontal position of the fixation target on the display. Traces are aligned at the onset of the fixation target (inverted triangles). L, left; R, right. (B) Horizontal eye positions during leftward (left) and rightward (right) saccades. Traces are aligned at the shift of the fixation target (inverted triangles).

In the blocked-design fMRI, fixation trials and serial saccade trials were presented in alternating blocks of trials. In the fixation trials (Figure 1A, lower), the animals maintained central fixation accurately with a standard deviation of the eye positions of  $0.15 \pm 0.03$  degrees in visual angle (mean  $\pm$  SD for three animals). In the serial saccade trials (Figure 1A, upper), the animals sequentially made a horizontal saccade in response to the shift of the fixation target, with a proportion correct of  $99.4\% \pm 0.4\%$  and a latency of  $204.7 \pm 15.9$  ms (Figure 1B). During the postsaccadic fixation period, the standard deviation of the eye positions was  $0.18 \pm 0.08$  degrees. The range of the trial length was 3.5–5.5 s, and there were intertrial intervals of 2–3 s. In the event-related fMRI, animals were required to make a horizontal visually guided saccade up to three times within a trial. The proportion correct was  $94.7\% \pm 0.7\%$ , latency was  $220.3 \pm 11.3$  ms, and the standard deviation of the eye position during the postsaccadic fixation period was  $0.25 \pm 0.18$  degrees. With the use of plastic head-holding devices, motion of the monkey head during the functional data acquisition was minimal: drifts were less than 0.2 mm, and rotations were less than 0.3 degrees.

#### **Cortical Regions Activated during Visually Guided Saccades**

The group analysis of the blocked-design fMRI data led to visualization of a distributed neural system in the dorsal frontoparietal network subserving saccadic eye control (Figure 2; Table 1).

In the posterior parietal cortex, significant BOLD activations were clustered along the banks of the intraparietal sulcus, mainly in BA 7 (Figure 2A). There were multiple pairs of bilateral peaks from the fundus to the lateral bank of the intraparietal sulcus (Figure 2B). We call a pair of bilateral activity peaks “homotopic” (see Experimental Procedures). The most dorsally located one is likely situated in area LIPd (dorsal lateral intraparietal), whereas ventrally located ones are possibly in areas LIPv (ventral lateral intraparietal) or VIP (ventral intraparietal) (Seltzer and Pandya, 1986; Colby et al., 1993; Andersen et al., 1997; Lewis and Van Essen, 2000). In this paper, we tentatively label these peaks “LIPv” and “LIPv/VIP,” respectively. Close to the LIPd, activity was also situated on the lateral surface of the inferior parietal lobule (area 7a). A distinctive homotopic peak was also found at the posterior tip of the parietal convexity near the junction of the intraparietal, parietooccipital, and lunate sulci. The BOLD signal was mapped both in area DP (dorsal preunate) lateral to the intraparietal sulcus (Andersen et al., 1990; Lewis and Van Essen, 2000) and in the adjacent cortex dorsomedial to the intraparietal sulcus (Nakamura et al., 1999; Snyder et al., 2000). We tentatively call this spot “area DP.” Homotopic peaks were also located more anteriorly in area 7a/7b and in area AIP. Unilateral activations were found close to the homotopic peaks near the intraparietal sulcus and were also situated in the posterior cingulate sulcus.

In the frontal cortex, the peak of saccade-related BOLD activity was bilaterally located in the banks of the arcuate sulcus (Figures 2A and 2D), approximately in BA 8. This region would correspond to the FEF as defined by electrophysiology and microstimulation studies in macaque monkeys (Bruce et al., 1985; Schall, 1997; Tehovnik et al., 2000). Unexpectedly, homotopic peaks were also observed in the premotor areas (PMv and PMd) in BA 6 near the posterior spur of the arcuate sulcus (Figure 2A). Significant activations were also found in the region of posterior principalis near the posterior end of the principal sulcus, approximately in BA 46/8.

#### **Modulation of BOLD Activity by Saccade Directions**

Then, in event-related fMRI experiments, we compared the BOLD signal changes in response to leftward and rightward saccades (Figure 3). To quantitatively estimate the bias of BOLD signals to contraversive saccades compared with ipsiversive saccades, we defined “contraversive selectivity” in functionally defined ROIs based on the blocked-design results (see Experimental Procedures). We found that, in most ROIs, the contraversive selectivity showed significant direction preference ( $p < 0.05$ , Wilcoxon signed rank test; Table 1). Among the parietal homotopic ROIs, the contraversive selectivity was highest in LIPd ( $z = 8.2$ ) (Figure 3B). Dorsally located regions (LIPd and 7a) tended to show higher selectivities than ventrally located regions (LIPv and LIPv/VIP). Among the frontal homotopic ROIs, FEF showed the highest contraversive selectivity ( $z = 4.8$ ), and premotor areas showed low selectivities. In the unilaterally activated peaks in the frontal and parietal cortices, the contraversive selectivities were similar to those of nearby homotopic peaks (Table 1).

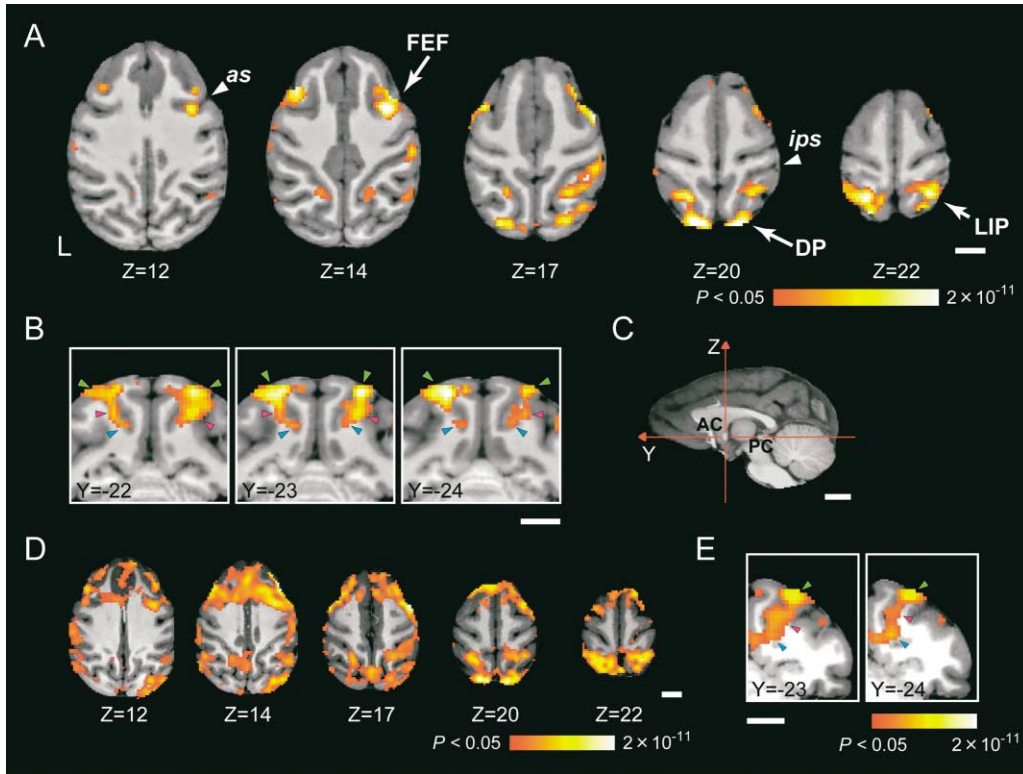


Figure 2. BOLD Activity Associated with Saccade in Monkeys

(A) Saccade-related activity in monkeys revealed by the group analysis. Activity map is superimposed on transverse sections of the normalized structural MRI (thresholded at  $p < 0.05$ , corrected for multiple comparisons). At the bottom of each image is indicated the z coordinate in the bicommissural space. FEF, frontal eye field; LIP, lateral intraparietal; DP, dorsal prelunate; as, arcuate sulcus; ips, intraparietal sulcus; L, left. (B) Multiple activity peaks along the intraparietal sulcus revealed by the group analysis. Activity map is superimposed on coronal MRI sections (thresholded at  $p < 0.05$ , corrected for multiple comparisons). At the bottom left corner of each image is indicated the y coordinate in the bicommissural space. Arrow heads indicate activation peaks: green, dorsal lateral intraparietal (LIPd); magenta, ventral lateral intraparietal (LIPv); blue, ventral lateral intraparietal/ventral intraparietal (LIPv/VIP). (C) Sagittal MRI section showing the origin and axes of the monkey bicommissural space (Nakahara et al., 2002). AC, anterior commissure; PC, posterior commissure. (D) Saccade-related activity in a single subject. Saccade-related activity was analyzed in a single monkey subject and superimposed on the transverse sections of the individual structural MRI (thresholded at  $p < 0.05$ , corrected by FDR). (E) Multiple activity peaks along the intraparietal sulcus in a single subject. Activities in two contiguous coronal sections at the level of intraparietal sulcus are shown (thresholded at  $p < 0.05$ , corrected by FDR). Arrow heads are denoted as in (B). Color scales (A, D, and E) indicate p values. Scale bars (A–E), 10 mm. Left-right direction of the brain images conforms to that of the figure (A, B, D, and E).

### Human fMRI Studies

#### Cortical Regions Activated during Visually Guided Saccades

We conducted functional scanning of healthy human subjects with a 1.5 T MRI scanner, using the same task sequence and visual stimuli as in the monkey experiments. A random effect analysis of the blocked-design fMRI data showed significant activations related to saccadic eye movements in dorsal cortical regions including the frontal and posterior parietal cortex (Figure 4A).

In the parietal cortex, two pairs of homotopic peaks were distinguished along the intraparietal sulcus in the superior parietal lobule, approximately in BA 7 (Table 2). The first one, anterior SPL, was located anteriorly near the junction of the intraparietal and the postcentral sulci. The second one, posterior SPL, was located at a more posterior and superior position. Another pair of activity peaks, IPS/TOS, was located near the border of the parietal and occipital cortex, just superior to the posterior end of the intraparietal sulcus where it meets the transverse occipital sulcus. Outside the parietal cor-

tex, homotopic regions were also situated in the visual areas and in the cerebellum.

In the frontal cortex, there was a large body of activations occupying the banks of the precentral sulcus (PrCS), which continued to the superior frontal sulcus (SFS) and the medial wall of the frontal cortex. We tentatively identified four pairs of homotopic peaks within this cluster (Table 2): PrCS/SFS, located at a medial position in the cluster near the junction of the precentral and the superior frontal sulci; inferior PrCS, located at an inferior and lateral position in the cluster near the lip of the precentral sulcus; superior PrCS, located at a superior and posterior part of the precentral sulcus; and MeFG (medial frontal gyrus), on the medial wall of the frontal gyrus.

#### Modulation of BOLD Activity by Saccade Directions

ROI analysis of the human event-related fMRI data revealed a characteristic distribution of contraversive selectivities across different cortical areas both in the parietal and frontal lobes (Table 2; Figure 4C). In the

Table 1. Brain Regions Activated in Monkeys

Hemisphere	Group			t Value	Homotopic Regions	CS	Individuals			
	Coordinates						t Value			
	X	Y	Z				M1	M2	M3	
<b>Frontal</b>										
L	-16	6	18	7.4	] FEF	4.8*	4.5	5.2	4.7	
R	14	5	14	9.2			6.3	6.4	5.0	
L	-15	12	14	7.6	] posterior principalis	2.9*	6.0	6.2	2.9	
R	16	10	13	8.3			8.3	8.2	5.8	
L	-20	2	17	5.5	] PMv	2.5*	3.9	5.6	-	
R	19	2	17	7.9			4.7	7.5	5.6	
L	-13	10	18	5.4	] PMd	1.5	2.7	7.9	-	
R	12	11	18	6.6			4.2	4.7	4.6	
R	13	4	21	6.8			1.0	2.8	5.5	4.5
L	-24	-1	9	6.0		n.d.	4.3	4.6	2.7	
L	-22	-1	15	5.3		1.4	5.9	-	-	
L	-21	9	10	4.8		n.d.	6.1	3.4	-	
L	-2	13	20	4.7		1.5	-	6.0	4.8	
<b>Parietal</b>										
L	-9	-24	22	8.4	] LIPd	8.2*	5.7	6.8	5.6	
R	11	-23	22	7.9			3.8	6.8	-	
L	-16	-20	22	5.7	] 7a	7.9*	4.0	4.4	5.9	
R	14	-21	19	6.2			4.6	4.8	8.2	
L	-6	-23	13	5.3	] LIPv/VIP	4.4*	3.5	-	3.4	
R	8	-24	14	5.1			4.5	2.3	-	
L	-9	-22	16	5.8	] LIPv	3.5*	3.6	3.7	3.1	
R	11	-22	16	6.5			5.2	4.6	4.5	
L	-20	-16	20	4.8	] 7a/7b	4.3*	4.2	2.8	4.3	
R	20	-15	17	6.2			5.9	3.5	4.1	
L	-22	-7	16	4.6	] AIP	3.8*	4.9	3.4	-	
R	22	-8	15	6.5			6.1	4.8	-	
R	10	-27	22	6.5			7.8*	5.1	5.7	6.3
L	-4	-25	22	6.2		6.2*	3.5	6.1	4.6	
R	7	-19	23	5.5		n.d.	2.6	4.3	4.0	
R	21	-11	18	5.5		1.6	-	4.6	2.9	
R	15	-17	18	5.0		5.2*	2.8	3.5	-	
L	-24	-8	13	4.9		3.6*	5.3	4.2	-	
<b>Parietooccipital</b>										
L	-8	-33	19	9.6	] DP	3.0*	6.4	8.3	5.2	
R	8	-32	19	8.7			5.5	7.3	5.4	
L	-3	-34	19	7.8		0.2	4.9	7.1	4.5	
<b>Temporal</b>										
L	-22	-25	14	4.5	] V4t/V4	1.0	4.6	4.1	3.8	
R	20	-25	15	5.6			4.1	4.5	-	
R	16	-27	17	5.9		4.6*	4.6	3.6	5.7	
R	22	-21	15	5.3		4.1*	3.7	-	-	
L	-20	-20	11	4.7		3.4*	-	3.6	3.3	
L	-24	-19	11	4.6		n.d.	2.9	3.9	3.3	
<b>Occipital</b>										
L	-15	-31	9	3.8 <sup>†</sup>	] V3/V3A	n.d.	n.d.	4.2	-	
R	13	-33	13	4.8			3.2	5.9	-	
R	17	-33	15	4.9			1.2	3.2	5.0	2.7
R	5	-25	10	4.7			5.8*	-	2.7	4.0

Significant peaks at a voxel level of  $p < 0.05$  corrected for multiple comparisons. Coordinates are listed in monkey bicommissural space (Nakahara et al., 2002). FEF, frontal eye field; PMv, ventral premotor; PMd, dorsal premotor; LIPd, dorsal lateral intraparietal; LIPv, ventral lateral intraparietal; VIP, ventral intraparietal; 7a, area 7a; 7b, area 7b; AIP, anterior intraparietal; DP, dorsal prelunate; V4, visual area 4; V4t, V4 transitional area; V3, visual area 3; V3A, visual area V3A; L, left; R, right; CS, contraversive selectivity; n.d., not defined.

<sup>†</sup>Data were obtained from two subjects (M2 and M3). \*Significant at  $p < 0.05$  (Wilcoxon signed rank test).

intraparietal regions, neural activity showed significant bias toward contraversive saccades in posterior SPL ( $z = 3.0$ ;  $p < 0.003$ , Wilcoxon test), but not in anterior SPL ( $z = 1.2$ ;  $p > 0.2$ ). The ROI near the parietooccipital border (IPS/TOS) showed strong contraversive selectivity ( $z = 3.3$ ;  $p < 0.001$ ). In the frontal cortex, the region at the intersection of the precentral and the superior

frontal sulci (PrCS/SFS) showed the highest selectivity to contraversive saccades ( $z = 2.6$ ;  $p < 0.02$ ). Contraversive selectivity reached significance in MeFG ( $z = 2.1$ ;  $p < 0.04$ ) but not in superior PrCS ( $z = 1.6$ ;  $p > 0.1$ ). Regions in the inferior precentral sulcus (inferior PrCS) had the lowest contraversive bias among the human homotopic regions ( $z = 0.4$ ;  $p > 0.6$ ).

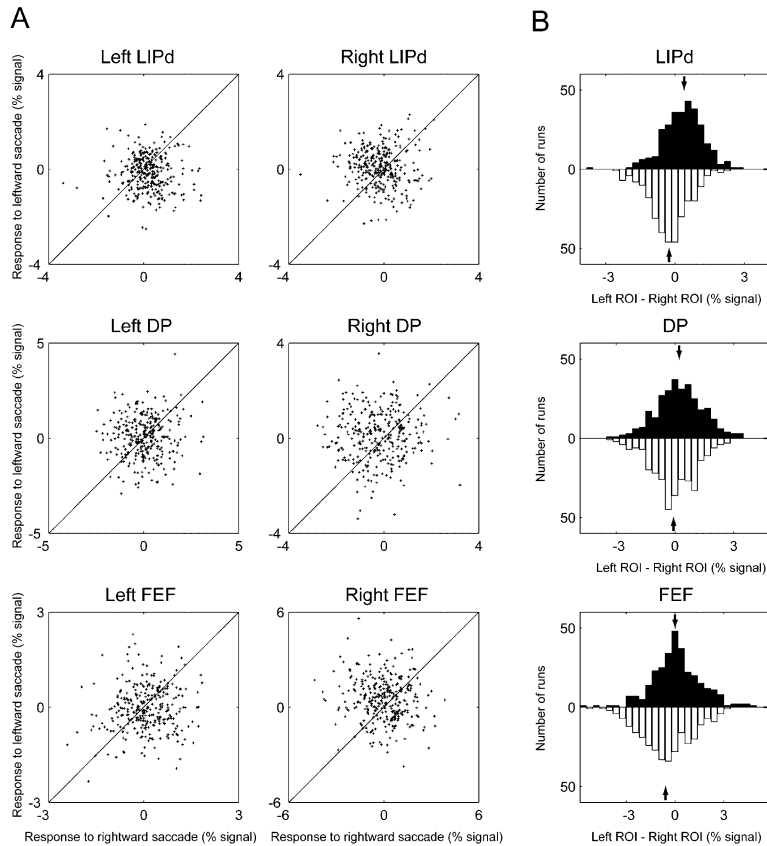


Figure 3. Modulation of BOLD Activity by Directions of Saccades in Monkeys

(A) BOLD activity in response to rightward saccades (horizontal axis) and to leftward saccades (vertical axis) for individual runs, represented as scattergrams. Data for left and right homotopic ROIs are shown in the left and right column, respectively. Each row represents data for LIPd, DP, and FEF (from top to bottom).

(B) Histograms showing number of runs sorted by activity difference (percent signal) between the left and the right homotopic ROIs during rightward (filled bars) and leftward (open bars) saccades. Arrows indicate the median of the distributions.

### Comparisons between Saccade and Visual Components

To examine the possible contribution of the peripheral visual stimuli to the observed activity, we conducted control experiments in which visual stimulation parameters were matched to those in the original saccade task, but no saccade was performed. In both monkeys and humans, the BOLD signal increases in most frontal and parietal homotopic regions were larger in the saccade condition than in the control condition, but those in early visual regions were comparable between the two conditions (Figure 5A for monkeys, Figure 5B for humans). We evaluated the responses across different homotopic regions during the saccade and control conditions using two-way ANOVA. In both monkeys and humans, there were significant main effects of CONDITION (monkeys,  $p < 0.0001$ ; humans,  $p < 0.0001$ ) and REGION  $\times$  CONDITION interactions (monkeys,  $p < 0.0001$ ; humans,  $p < 0.004$ ). Multiple comparisons revealed that the frontal and parietal homotopic regions showed significantly larger responses in the saccade condition than in the control condition: FEF, posterior principalis, PMv, PMd, LIPd, 7a, LIPv/VIP, LIPv, 7a/7b ( $p < 0.01$ ; Tukey's test), and AIP ( $p < 0.028$ ) in monkeys; PrCS/SFS, MeFG, superior and inferior PrSC, and posterior and anterior SPL in humans ( $p < 0.004$ ). We also performed the same statistical analysis using relative BOLD signal changes normalized with those in the occipital regions (see Experimental Procedures). Again, significant main effects of CONDITION (monkeys,  $p < 0.0001$ ; humans,  $p < 0.0001$ ) and REGION  $\times$  CONDITION

interactions (monkeys,  $p < 0.001$ ; humans,  $p < 0.0001$ ) were obtained. Significantly larger responses in the saccadic condition than in the control condition were also shown by multiple comparisons in the frontal and parietal regions listed above (monkeys,  $p < 0.034$ ; humans,  $p < 0.002$ ) except AIP in monkeys. These results indicated that activity associated with visually guided saccades in the above-mentioned frontal and parietal regions have significant oculomotor components.

### Discussion

In the present study, we have provided direct evidence of the functional correspondences of the cortical eye fields between macaques and humans by using a common technology (BOLD fMRI) and identical oculomotor paradigms. In the dorsolateral frontal cortex, BOLD peaks were mapped in FEF (BA 8), premotor areas (BA 6), and posterior principalis regions (BA 46/8) in monkeys and in multiple regions along the precentral sulcus (BA 6), including the intersection with the superior frontal sulcus (near BA 6/8 border), in humans (Figures 6A and 6B). Thus, the saccade-related BOLD signal was distributed in overlapped frontal regions across the two species. In the posterior association cortex, activity was situated in the lateral bank of the intraparietal sulcus (LIPd, LIPv, LIPv/VIP) and areas 7a, 7a/7b, AIP, DP in monkeys and in the posterior and anterior SPL regions and IPS/TOS in humans (Figures 6C and 6D). By interspecies comparison of the BOLD activation locus and its contraversive selectivity, we propose that the human

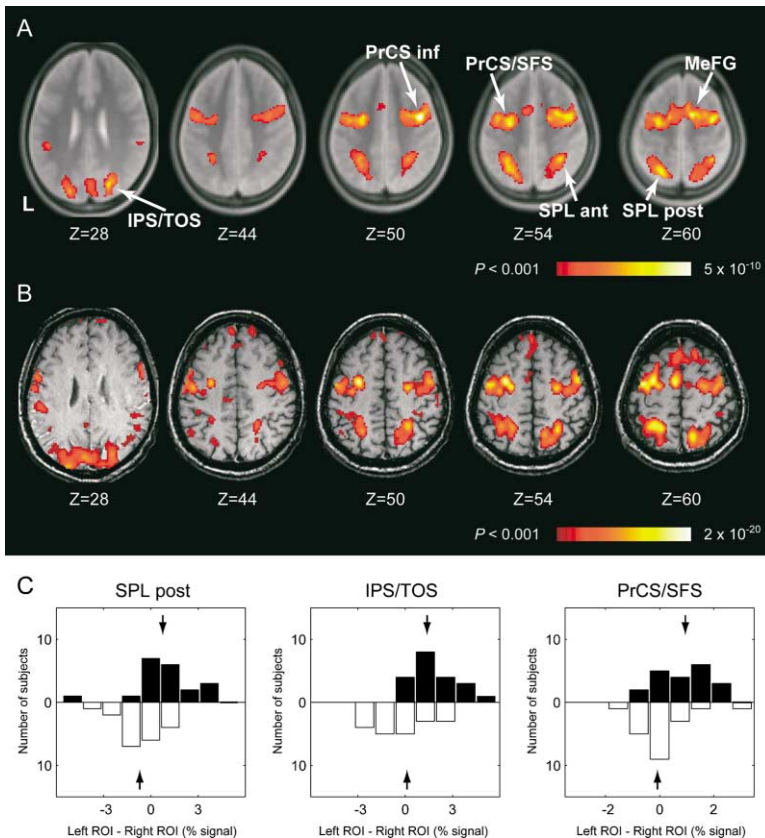


Figure 4. BOLD Activity Associated with Saccade in Humans

(A) Saccade-related activity in humans revealed by the group analysis. Format is as in Figure 2. At the bottom of each image is indicated the z coordinate in MNI space. PrCS, precentral sulcus; SFS, superior frontal sulcus; MeFG, medial frontal gyrus; SPL, superior parietal lobule; IPS, intraparietal sulcus; ant, anterior; post, posterior; inf, inferior. (B) Saccade-related activity in a single subject. Saccade-related activity was analyzed in a single human subject and superimposed on transverse sections of the individual T1-weighted structural MRI. (C) Histograms showing number of subjects sorted by activity difference in the homotopic ROIs between rightward and leftward saccades. Format is as in Figure 3B. Color scales (A and B) indicate p values. Left-right direction of the brain images conforms to that of the figure (A and B).

PrCS/SFS is functionally similar to the macaque FEF and that the human posterior SPL is similar to the macaque LIPd. These correspondences are basically compatible with what has been proposed by Petit et al., Sereno et al., and other authors (Sweeney et al., 1996; Petit et al., 1997; Courtney et al., 1998; Beauchamp et al., 2001; Sereno et al., 2001; Rosano et al., 2003). In the following, we will discuss individual activation peaks and attempt to give a detailed account of the functional correspondence of the cortical organization for saccadic eye control in primates.

#### Eye Fields in the Posterior Association Cortex

BOLD activity in the monkey parietal cortex was clearly situated along the banks of the intraparietal sulcus (Figure 2B), where the population of neurons exhibited oculomotor-related activity and intracortical microstimulation evoked saccades (Andersen et al., 1997; Colby and Goldberg, 1999). Multiple peaks were distinguished from the fundus to the lateral bank of the intraparietal sulcus, not only in the group analysis, but also in the individual analysis (Table 1). These locations possibly corresponded to areas LIPd, LIPv, and LIPv/VIP (Seltzer and Pandya, 1980, 1986; Andersen et al., 1997; Lewis and Van Essen, 2000) that have been identified based on immunohistochemistry, cyto- and myeloarchitecture, connectivity, and physiological properties. We also found activity in the parietooccipital cortex near the junction of the intraparietal, parietooccipital, and lunate sulci (Figures 2A and 6C). The activation appeared to include area DP on the lateral surface where saccade-

related neuronal activity was reported (Andersen et al., 1990) as well as dorsal area 5 where neural activity is likely modulated by saccades (Snyder et al., 2000) and eye positions (Nakamura et al., 1999). The location was close to the parietooccipital border, and we could not exclude the possibility that part of the activation might fall on the most dorsal portion of the secondary visual cortex (area V2) in the occipital cortex. However, this possibility is less likely for two reasons. First, the monkeys made horizontal saccades to the fixation targets. Considering the retinotopic organization of macaque visual areas (Zeki, 1977; Gattass et al., 1981) that is also confirmed by fMRI mapping (Brewer et al., 2002), activity in V2, if any, should emphasize the representation of the horizontal meridian at the V2/V3 border in the fundus of the lunate sulcus rather than a representation of the vertical meridian near the V1/V2 border on the dorsal surface. But in our results, this was not the case. Second, it is reported that a BOLD signal at a field strength of 4.7 T can be accurately localized with the underlying neural site of activity (Logothetis et al., 2001, 2002) and is not seriously affected by perturbations such as vascular effects (Menon and Kim, 1999), although this issue is still under debate.

In the human parietal cortex, the widespread recruitment of regions in the SPL (Figure 4A), approximately in BA 7, was consistent with the results of previous neuroimaging studies using oculomotor paradigms (Corbetta et al., 1998; Luna et al., 1998; Pery and Zeki, 2000). Two distinct peaks, anterior SPL and posterior SPL, were bilaterally situated in the human SPL. Among

Table 2. Brain Regions Activated in Humans

Hemisphere	Coordinates (MNI)			Coordinates (Talairach)			t Value	Homotopic Regions	CS
	X	Y	Z	X'	Y'	Z'			
<b>Frontal</b>									
L	-26	-12	54	-24	-15	46	9.5	] PrCS/SFS	2.6*
R	18	-6	56	15	-9	49	9.2		
L	-14	-6	62	-13	-9	54	7.9	] MeFG	2.1*
R	12	-2	62	10	-5	54	11.5		
L	-24	-8	64	-22	-11	55	8.3	] PrCS sup	1.6
R	20	-4	66	17	-7	57	9.8		
L	-40	-8	52	-36	-11	45	7.8	] PrCS inf	0.4
R	40	-4	50	34	-7	43	13.5		
R	36	-6	62	31	-9	54	10.2		1.6
R	28	0	56	24	-3	49	9.1		0.2
L	-18	-14	62	-17	-17	53	7.4 <sup>†</sup>		1.7
L	-6	-4	66	-6	-7	57	7.3		0.2
<b>Parietal</b>									
L	-22	-62	60	-20	-63	49	9.2	] SPL post	3.0*
R	22	-62	60	19	-63	49	5.6 <sup>†</sup>		
L	-28	-58	54	-25	-60	44	8.0	] SPL ant	1.2
R	34	-50	56	29	-62	46	8.5		
<b>Parietooccipital</b>									
L	-22	-84	26	-20	-85	18	7.5	] IPS/TOS	3.3*
R	22	-78	28	19	-79	20	9.0		
<b>Temporal</b>									
R	44	-62	8	38	-63	4	10.0		1.4
L	-52	-70	2	-47	-71	-2	7.5		1.8
<b>Occipital</b>									
L	-28	-78	-10	-25	-79	-13	8.1	] Lingual	3.8*
R	28	-74	-8	24	-75	-11	7.5		
L	-16	-76	-8	-15	-77	-11	11.4	] Lingual	3.7*
R	12	-74	-12	10	-75	-15	10.1		
L	-12	-82	2	-11	-83	-3	9.6	] Calcarine	3.5*
R	8	-84	2	6	-85	-3	8.3		
L	-8	-72	0	-8	-73	-4	7.7	] Calcarine	3.3*
R	16	-76	0	13	-77	-4	11.9		
L	-12	-90	-2	-11	-91	-7	8.3		2.6*
L	-2	-84	6	-3	-85	1	7.5		2.4*
<b>Thalamus</b>									
L	-14	-24	12	-13	-27	9	7.3		0.4
<b>Cerebellum</b>									
R	-8	-76	-18	-8	-77	-20	7.5	] Cerebellum	1.3
R	10	-72	-20	8	-73	-22	8.7		
R	24	-74	-18	20	-75	-20	11.8		
R	34	-64	-24	29	-65	-25	8.8		

Significant peaks at a voxel level of  $p < 0.05$  corrected for multiple comparisons. Coordinates are listed in MNI space and also in Talairach and Tournoux (1988) atlas space using coordinate transformation program (<http://www.mrc-cbu.cam.ac.uk/Imaging/Common/mnispace.shtml>). PrCS, precentral sulcus; SFS, superior frontal sulcus; MeFG, medial frontal gyrus; SPL, superior parietal lobule; IPS, intraparietal sulcus; TOS, transverse occipital sulcus; L, left; R, right; CS, contraversive selectivity; n.d., not defined.

<sup>†</sup>The distance between this peak and (18, -6, 56) is the same as the distance between (-26, -12, 54) and (18, -6, 56). Coordinates are in MNI space. <sup>\*</sup>Significant only at a cluster level of  $p < 0.05$  corrected for multiple comparisons. <sup>\*</sup>Significant at  $p < 0.05$  (Wilcoxon signed rank test).

them, the more posteriorly and superiorly located peaks (posterior SPL) showed higher neural selectivity to the directions of saccade (Table 2). This result was comparable to the finding from our monkey study that the more dorsally situated peaks, including some unilateral regions, exhibited higher contraversive selectivity (Table 1). From these observations, our study adds functional evidence that the human posterior SPL might be similar to the monkey LIPd (Figures 6C and 6D). This view is consistent with a finding from a human imaging study that singularity of preferred directions lying in the posterior portion of the SPL may correspond to the “putative” human LIP (Serenio et al., 2001). However, other independent studies are required to determine functional correspondences, because existing anatomical evi-

dence is divergent for interspecies correspondences of IPL and SPL in primates (Brodmann, 1905; Von Bonin and Bailey, 1947).

In the regions near the parietooccipital junction, saccade-related BOLD activity was found in monkeys (area DP) and humans (area IPS/TOS). However, monkey DP was different from human IPS/TOS in two respects. First, in monkey DP, the signal changes during the saccade condition were significantly larger than during the visual control condition ( $p < 0.0001$ , ANOVA, Tukey's test), whereas in human IPS/TOS, the signal changes were not significantly different between the two conditions ( $p = 0.0528$ ). This suggests that, unlike in monkey DP, activity in human IPS/TOS may largely be accounted for as a response to the visual stimulus. Second, human

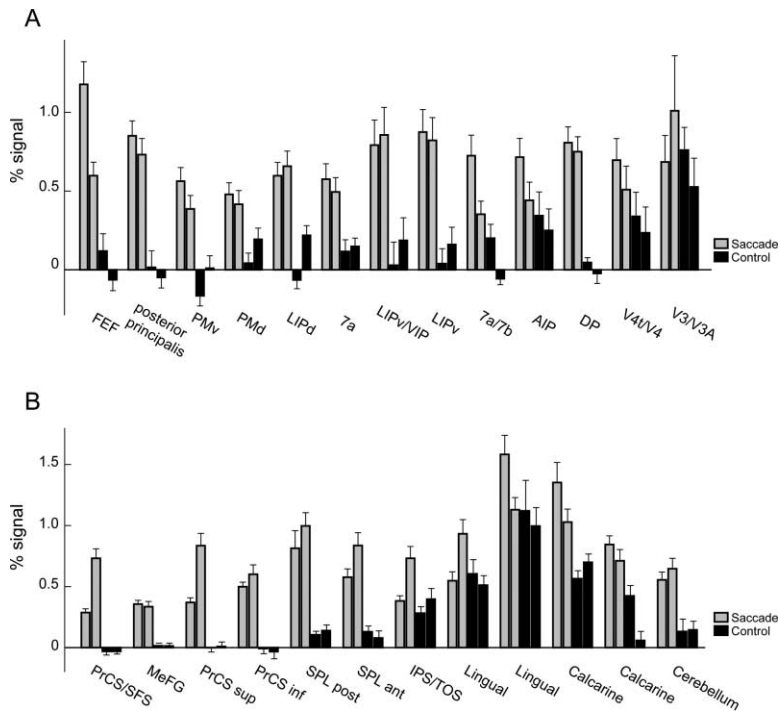


Figure 5. Comparisons of BOLD Signal Changes in the Homotopic Regions Between the Saccade and Visual Control Condition

Percent signal changes in the saccade (gray bars) and control condition (black bars) in monkeys (A) and humans (B) are plotted. Four bar plots in each column indicate, from left to right, the signal changes in the homotopic ROI of the right hemisphere in the saccade condition, those of the left hemisphere in the saccade condition, those of the right hemisphere in the control condition, and those of the left hemisphere in the control condition. The signal changes were taken from the voxel that showed the maximal t value in each ROI. FEF, frontal eye field; PMv, ventral premotor; PMd, dorsal premotor; LIPd, dorsal lateral intraparietal; LIPv, ventral lateral intraparietal; VIP, ventral intraparietal; 7a, area 7a; 7b, area 7b; AIP, anterior intraparietal; DP, dorsal pre-lunate; V4, visual area 4; V4t, V4 transitional area; V3, visual area 3; V3A, visual area V3A. PrCS, precentral sulcus; SFS, superior frontal sulcus; MeFG, medial frontal gyrus; SPL, superior parietal lobule; IPS, intra parietal sulcus; TOS, transverse occipital sulcus. Error bars indicate standard errors.

IPS/TOS showed the strongest bias toward contraversive saccade among the parietal regions (Table 2), while the monkey area DP showed the weakest (Table 1). Thus, it is difficult to determine the functional correspondences of the homotopic regions near the parietooccipital border between the two species. One possibility is that the monkey counterpart of human IPS/TOS and human counterpart of monkey DP might have shown subthreshold activity in our experiment. It should be noted that our assignment of “area DP” to the activity peak in the monkey posterior parietal tip is only tentative, and the region could be further divided into functionally distinct subdivisions.

### Eye Fields in the Frontal Cortex

In the monkey frontal cortex, the activity peak in the banks of the arcuate sulcus would correspond to the FEF as defined by intracortical microstimulation studies in macaques (Bruce et al., 1985; Schall, 1997; Tehovnik et al., 2000). The dorsoventral level of the activation was centered approximately at the intersection of the arcuate sulcus and the posterior extension of the principal sulcus. Given the amplitudes of the horizontal saccades in our study (5.5 to 11 degrees), this location is consistent with the topographical organization of FEF revealed with single-unit recording and microstimulation studies (Suzuki and Azuma, 1983; Bruce et al., 1985).

The extent of BOLD activation during the visually guided saccades in our study, which we tentatively call “FEF+,” was not restricted in the extent of microstimulation-defined FEF in monkeys, which we call “FEF proper.” FEF+ extended far more posteriorly than we had expected to other peaks that were located in premotor areas (BA 6) near the posterior spur of the arcuate sulcus (Figure 6A). Since no prominent activation was found in the primary motor cortex, it is not likely that

activity in the premotor areas could be attributed to task-irrelevant body movements coincidentally correlated with the block cycle. Our finding that FEF+ involves premotor areas (BA 6) has two implications. First, this finding is consistent with some microstimulation and single-unit recording studies indicating neural activity related to saccade in the macaque premotor area (Preuss et al., 1996; Wise et al., 1997; Fujii et al., 1998; Ohbayashi et al., 2003). Second, our finding suggests considerable anatomical overlap of oculomotor representation in the macaque and human frontal cortex. Therefore, although the Brodmann area assigned to the human FEF by neuroimaging studies (BA 6) appears different from what is assigned to the macaque FEF by microstimulation studies (BA 8), the apparent interspecies difference could have been overemphasized.

As shown in the present study, saccade-related regions in the human precentral sulcus as revealed by many imaging studies (Paus, 1996; Petit et al., 1997; Astafiev et al., 2003) extended along the superior-inferior and medial-lateral axis, which might be a heterogeneous mixture of functionally different fields (Paus, 1996; Petit et al., 1997; Corbetta et al., 1998; Petit and Haxby, 1999). We propose that the human PrCS/SFS near the intersection of the precentral sulcus and the superior frontal sulcus would be functionally equivalent to the monkey FEF proper, because both areas are situated close to the border of BA 6 and BA 8 and show the highest neural selectivity for contraversive saccades in the frontal cortex (Figures 6A and 6B). Human inferior PrCS near the posterior bank of the precentral sulcus could possibly be functionally similar to the monkey premotor areas, since both areas are situated in the middle of BA 6 and exhibit relatively low contraversive selectivity.

Consistent with previous imaging studies that have argued that human supplementary eye fields (SEF) are

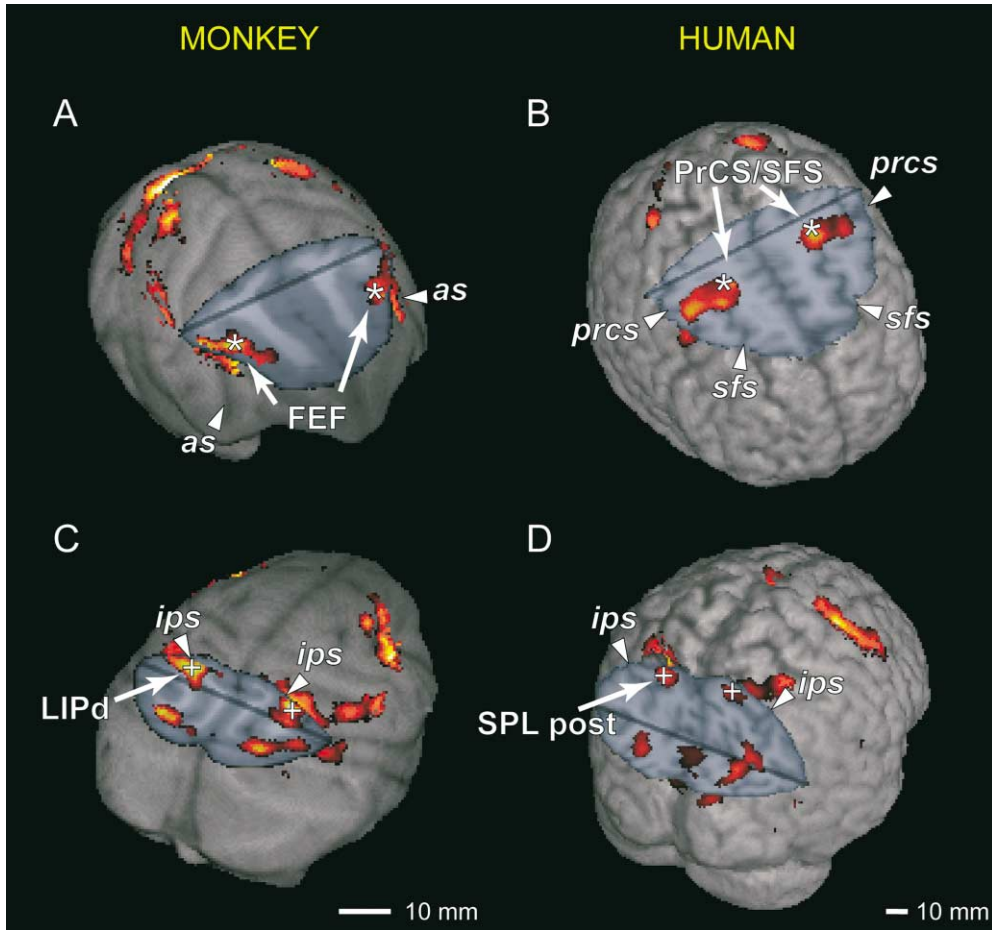


Figure 6. Saccade-Related Activity Superimposed on 3D-Rendered Brain Images

Monkey (A and C) and human (B and D) brain images are cut to show activity buried in the sulci in the frontal (A and B) and posterior parietal (C and D) cortex. Asterisks and crosses indicate homotopic regions showing the highest contraversive selectivity in the frontal and parietal cortex, respectively. FEF, frontal eye field; LIPd, dorsal lateral intraparietal; PrCS, precentral sulcus; SFS, superior frontal sulcus; SPL, superior parietal lobule; as, arcuate sulcus; ips, intraparietal sulcus; prcs, precentral sulcus; sfs, superior frontal sulcus; post, posterior.

in fact on the medial wall (Luna et al., 1998; Grosbras et al., 1999; Merriam et al., 2001; Picard and Strick, 2001), we found activity in the human MeFG. In the present study, the monkey SEF (Schlag and Schlag-Rey, 1987; Schall, 1997) was not robustly activated in the group data, although activity was observed in some individuals (Figure 2D). The reason why the monkey SEF activity did not reach significance bilaterally at the population level is likely explained by two factors. First, it has been suggested that neural activity in SEF decreases as subjects become habituated to the task through learning and experience in both humans (Sakai et al., 1998) and monkeys (Chen and Wise, 1995). In this sense, our monkeys were experts who were overtrained in the oculomotor tasks for months, whereas the human participants were novices without any experience prior to the scanning. To test this possibility, we compared saccade metrics across the two species. Saccade errors in the monkey ( $0.43 \pm 0.05$  degrees for small saccades,  $0.72 \pm 0.18$  degrees for large saccades; mean  $\pm$  SD) were significantly smaller ( $p < 0.0001$ ; ANOVA) than in humans

( $1.28 \pm 0.37$  degrees for small saccades,  $1.45 \pm 0.41$  degrees for large saccades). This may be due to training differences across the two species. However, the direct comparison of saccade metrics across the two species may need some reservations, because monkeys' heads were much more firmly immobilized with head holders, and the resolution of eye position monitoring was finer for them than for humans. As far as we examined within human subjects, saccade errors were not significantly correlated with MR signal changes in the MeFG ROIs ( $p > 0.16$ ). Second, since the monkey SEF is one of the structures situated farthest from the AC-PC plane, a currently available registration algorithm might not be accurate enough to compensate for the variability of individual monkey brains.

#### Methodological Considerations

Prior electrophysiological studies using macaque monkeys suggested that discharges of single neurons reflect several different aspects of the visually guided saccade in the FEF (Bruce and Goldberg, 1985; Tehovnik et al.,

2000) and posterior parietal areas (Andersen et al., 1997). These include presaccadic motor preparation and visual attention, saccade execution, or postsaccadic processing such as corollary discharge (Sommer and Wurtz, 2002) or evaluation of the new eye position in the orbit (Colby and Goldberg, 1999). The BOLD signal changes associated with visually guided saccades would be a mixture of these heterogeneous neural processes.

Our visual control experiments in monkeys and humans (Figure 5) confirmed that activities associated with visually guided saccades in frontal and parietal regions, except human IPS/TOS, were not solely caused by visual stimulation but were significantly related to saccade performance. It is noteworthy that Corbetta et al. reported that attentional mechanisms are automatically recruited by the shifts of the targets during visually guided saccades (Corbetta et al., 1993). Therefore, although our results confirmed that activity in frontal and parietal areas was not solely caused by pure visual stimulation, this does not exclude the possibility that the activity was associated with automatically recruited attentional mechanisms. It would be interesting to further dissociate oculomotor and attentional components of the activity in each ROI by using other behavioral paradigms such as delayed saccade, antisaccade, or double-step saccade.

The extent of the monkey FEF+ defined by our BOLD fMRI study appears larger than the extent of the FEF proper defined by intracortical microstimulation studies. This does not mean that fMRI mislocalizes neuronal activity. The extent of microstimulation-defined FEF is not identical with that defined by single-unit recordings. Moreover, Logothetis and coworkers reported that BOLD fMRI signals correlate well with local field potentials rather than extracellularly recorded action potentials (Logothetis et al., 2001). Thus, it is obvious that the spatial extent of FEF depends on the way by which it is defined.

Functional lateralization of the attentional system in the human parietal cortex has been suggested in both lesion and imaging studies (Driver and Mattingley, 1998; Mesulam, 1999; Perry and Zeki, 2000). In our human study, no suprathreshold activations were found in the right temporoparietal junction regions (Corbetta et al., 2000; but see Astafiev et al., 2003). Laterality of the cortical organization for the oculomotor control, particularly in humans, remains an important issue.

Based on the anatomical locations of BOLD activations and their selectivity to saccade directions, we found considerable similarities in the cortical organization for oculomotor controls in macaques and humans. Our results indicate that the well-known discrepancy of cytoarchitectonic areal assignment of the human FEF (BA 6) and the monkey FEF (BA 8) might have been attributable in part to methodological issues. In the human, a region at the junction of the precentral sulcus and the superior frontal sulcus would be putatively equivalent to monkey FEF, and a region in the posterior part of the superior parietal lobule would be putatively equivalent to monkey LIPd. These findings impose significant constraints in understanding the evolution of the cerebral association cortex in primates.

## Experimental Procedures

### Monkey fMRI Studies

#### Animals

We used three macaque monkeys (*Macaca fuscata*; M1, M2, M3; one female and two males) weighing 4–6 kg. All the experimental protocols were in full compliance with the regulations of the University of Tokyo School of Medicine and with the NIH guidelines for the care and use of laboratory animals. Before fMRI scanning, MR-compatible custom-made ceramic screws (zirconium oxide, Kyocera, Kyoto) and plastic head holders were implanted in the monkeys. Surgery was conducted in aseptic conditions under general anesthesia with sodium pentobarbital (5 mg/kg/h).

#### 4.7 T fMRI Acquisition

To obtain BOLD signal, we used a 4.7 T MRI scanner (Biospec 47/40, Bruker, Ettlingen) and 50 mT/m actively shielded gradient coils. During the imaging sessions, the monkey's head was fixed with the head holders to make the relative head position to the scanner constant. Multisegmented T2\*-weighted gradient-echo echo planar imaging (GE-EPI) was carried out, in which a segment of the K-space was scanned in a single step and the whole volume was scanned in multiple steps (Schmitt et al., 1998). In the blocked-design fMRI experiments, 16 segmented EPI were performed with an in-plane resolution of  $1 \times 1 \text{ mm}^2$ ; field of view (FOV),  $128 \times 128 \text{ mm}^2$ ; echo time (TE), 16.03 ms; time to repetition (TR), 346 ms per segment; flip angle (FA), 35 degrees; effective bandwidth, 108 kHz; ten contiguous transverse slices; and slice thickness, 2 mm (gapless). In the event-related fMRI experiments, 4 or 8 segmented EPI were performed with an inplane resolution of  $1 \times 1.25 \text{ mm}^2$  or  $1 \times 1 \text{ mm}^2$ ; FOV,  $64 \times 80 \text{ mm}^2$  or  $128 \times 128 \text{ mm}^2$ ; TE, 16.93 ms; TR, 625 ms per segment; FA, 40 or 45 degrees; effective bandwidth, 43.4 kHz or 67.9 kHz; seven contiguous transverse slices, slice thickness 2 mm; and interslice gap 0.5 mm. T1-weighted spin-echo images were also obtained in each experimental day for registration of EPI images. In separate sessions, high-resolution structural images of the monkeys were scanned using both the 3D-MDEFT (modified driven equilibrium Fourier transform) sequence (voxel =  $0.5 \times 0.5 \times 0.5 \text{ mm}^3$ ) and T1-weighted anatomical spin-echo sequence (voxel =  $1 \times 1 \times 1 \text{ mm}^3$ ).

#### Behavioral Procedures

The monkeys were trained on a fixation task and a serial saccade task, initially outside the magnet room. Then they were adapted to the posture and the noise during high-field fMRI scanning in a custom-made plastic chair (Nakazawa, Tokyo) and finally trained to perform the oculomotor tasks inside the magnet bore. In the fixation task, the monkeys were required to fixate on a white spot at the center of the display. If they maintained fixation throughout the trial for 3.5–5.5 s (varied across monkeys), they were rewarded with a drop of fruit juice. If the eye position deviated out of a fixation window (1.5 degree or less within the fixation spot), the trial was immediately aborted. Each trial was followed by an intertrial interval of 2–3 s. During the interval, the monkeys were not required to fixate, since no visual target was shown on the display. In the serial saccade task, fixation targets were sequentially presented from one position to the next up to ten times within a trial (Figure 1A). The position of the fixation target was pseudorandomly determined from three locations: the center of the display and positions 5.5 degrees left or right relative to the center. As the fixation target shifted, the animals were required to make a horizontal saccade to the new target. Thus, the amplitude of the visually guided saccade required was either 5.5 degrees (small saccade) or 11 degrees (large saccade). After the saccade, the animals were required to maintain fixation there for fixed (0.25 s or 0.75 s in blocked-design fMRI; see below) or variable (2–10 s in event-related fMRI) lengths of postsaccadic periods until the target was replaced with another one or disappeared at the trial end. The trial was aborted when the eye stayed in the prior fixation window for more than 400 ms after the shift or when the eye did not reach the new fixation window in 200 ms after leaving the old window. Behavioral performance was evaluated by proportion correct, saccade latency, and saccade errors. Here, proportion correct is defined as the probability that the monkey's eye reached the target window within the time limit described above.

In the magnet room, we used an infrared-sensitive CCD camera

with magnetic shield (XC-EI50, Sony, Tokyo) to monitor the eye positions. Spatial resolution of the eye-measurement system was approximately 0.1 degrees in visual angle. Online processing of eye position data, visual stimulus presentation, reward delivery, and MRI pulse trigger for task events were controlled with custom-made PC software (Hasegawa et al., 1998; Tomita et al., 1999). VGA visual signal was delivered to the magnet room via optic fibers, and visual stimuli were presented on a magnetically shielded 20-inch LCD monitor (Hitachi Medico, Tokyo).

#### **fMRI Scan Design**

We used a blocked-design fMRI paradigm to identify areas activated during the serial saccade task compared to the fixation task and used an event-related fMRI paradigm to examine modulation of the BOLD signals by saccade directions in the activated areas. This approach was adopted because the blocked design affords enhanced detection power (Liu et al., 2001), and the event-related design has the advantage of distinguishing responses sorted by trial types (Josephs and Henson, 1999). In the blocked paradigm, the fixation trials and serial saccade trials were presented in alternating blocks of two to six trials. In the serial saccade trial, the monkeys were required to successively make four to ten horizontal saccades in 3.5–5.5 s. Saccade and fixation blocks lasted for approximately 28–42 s and 14–21 s, respectively. One experimental run consisted of three to four saccade blocks and four to five fixation blocks in a total time of 240–288 s, during which 37–52 functional brain volumes were acquired. In the event-related paradigm, leftward and rightward saccades were interleaved with variable intervals of 2–10 s within or between trials. To accumulate neural activity associated with saccadic eye movements, two consecutive saccades with the same direction and amplitude were paired. One experimental run lasted for 210–360 s, during which 22–37 leftward and 22–37 rightward saccades were included, and 72–82 functional brain volumes were acquired.

#### **Data Analysis**

Data were analyzed with SPM99 (<http://www.fil.ion.ucl.ac.uk/spm/>) and custom-made MATLAB (Mathworks) software. Functional images were realigned and spatially normalized to a template that we made from 3D-structural images of one monkey's whole brain, with interpolation to a  $1 \times 1 \times 1$  mm space. This procedure enabled us to perform a group analysis of the monkeys and to introduce a stereotaxic coordinate arranged in bicommissural space in which the origin was placed at the anterior commissure (Nakahara et al., 2002). After normalization, the images were spatially smoothed with a Gaussian kernel (full width at half maximum 2 mm for the blocked-design experiments, 3 mm for the event-related experiments). We conducted voxel-wise statistical analysis based on the general linear model (GLM) using SPM99. In the blocked paradigm, sustained neural activity during each saccade block was modeled as a boxcar covariate of variable length in SPM99, and realignment parameters were also included in the model as covariates of no interest. A fixed-effect model was used for the group analysis of data from the three monkeys. We assessed statistical significance at a criterion of a single-voxel threshold of  $p < 0.05$  corrected for multiple comparisons (SPM99 default) across the brain volume examined. We excluded those peaks within 4 mm of another peak with higher  $t$  value. To confirm intersubject reproducibility of activated regions, we examined whether distinct peaks were located in individual monkeys within 4 mm of the activity peak of the group analysis (Table 1). A single-voxel threshold of  $p < 0.05$  corrected by the False Discovery Rate method (Genovese et al., 2002) was used for individual data analysis. Different correcting methods were applied to group and individual data because individual data had smaller degrees of freedom. Three-dimensional brain rendering and functional overlays were constructed using MRICro software (Rorden and Brett, 2000).

To define a homotopic pair of peaks, we used a nearest-neighbor algorithm (Burgund et al., 2003) as follows. First, we flipped the  $x$ -coordinates of all the peaks in the left hemisphere and superimposed them on the right hemisphere. Second, for each of the peaks derived from the left hemisphere, the nearest peak originally located in the right hemisphere was chosen and vice versa. If the nearest peaks from both hemispheres matched to each other and the distance did not exceed 5 mm, they were paired as homotopic peaks.

In the event-related fMRI, neural activity associated with leftward

or rightward saccades in response to the shift of the fixation spot was modeled as an event with the hemodynamic response function implemented in SPM 99. A leftward or rightward saccade to the initial fixation spot at the beginning of the trial was independently coded as a covariate of no interest. We localized the regions of interest (ROIs) using the statistical  $t$  map of the blocked-design fMRI: a ROI was functionally defined as those voxels within a 1 mm radius sphere around local peaks on the statistical map. We measured differential BOLD responses between left and right ROIs for each run and plotted histograms independently for leftward and rightward saccades (Figure 3B). Data from 100 runs were collected for each monkey. To evaluate whether the differential activity was larger for contraversive than ipsiversive saccades, we applied the Wilcoxon signed-rank test (Snedecor and Cochran, 1989) and defined the  $z$  score of the statistics as "contraversive selectivity." A larger score indicates that the activity tended to be more strongly correlated with contraversive than ipsiversive saccades. Contraversive selectivities for nonhomotopic ROIs were similarly calculated by pairing them with the voxels symmetrical to the midsagittal plane.

#### **Human fMRI Studies**

We conducted fMRI experiments with human subjects using the same task sequences and visual stimuli as in the monkey experiments. In human experiments, informed consent was obtained from 20 (nine female and 11 male) healthy right-handed subjects. They were scanned using experimental procedures approved by the institutional review board of the University of Tokyo School of Medicine. Functional MRI scans were performed on a 1.5 Tesla scanner as described previously (Konishi et al., 1998; Kikyo et al., 2002) with single-shot GE-EPI (FOV =  $256 \times 256$  mm<sup>2</sup>, TR = 4 s, TE = 50 ms, flip angle = 90 degrees, matrix =  $64 \times 64$ , slice thickness = 4 mm, 28 transverse slices). Functional images were realigned, spatially normalized to a template with interpolation to a  $2 \times 2 \times 2$  mm<sup>3</sup> space, and smoothed with a Gaussian kernel (FWHM 6 mm). Eye positions were measured with an infrared monitoring system (ISCAN, MA) (Gitelman et al., 2002) in separate sessions. Functional images from the 20 human participants were subjected to a GLM analysis (SPM99) and ROI analysis as in the monkey experiments. In human experiments, a random-effect model was used for estimating the data, since there were more subjects for the human study and more runs for the monkey study. Coordinates are listed in SPM-MNI space (<http://www.fil.ion.ucl.ac.uk/spm/>) and also in Talairach and Tournoux atlas space (Talairach and Tournoux, 1988) using a coordinate transformation program (<http://www.mrc-cbu.cam.ac.uk/Imaging/Common/mnispace.shtml>). We assessed statistical significance at a single-voxel threshold of  $p < 0.05$  corrected for multiple comparisons. We excluded those peaks within 8 mm of another peak with a higher  $t$  value. For the ROI analysis, data from ten runs was collected for each subject, and 3 mm radius sphere ROIs around local peaks were used. The homotopic ROIs were defined when the distance of the matched nearest peaks did not exceed 10 mm (round off to 1 mm place). Data from individual subjects, instead of individual runs, were used for the ROI analysis in the human study, since there were more subjects for the human study and more runs for the monkey study.

#### **Visual Control Experiments in Monkeys and Humans**

Two monkeys (M1 and M2 that were used in the saccade experiments) and 12 humans underwent blocked-design visual control experiments. During the ON epoch, visual stimuli matching spatial and temporal parameters of the visual targets in the original saccade task were presented, but no saccades were performed. During the OFF epoch, the subjects were required to actively maintain fixation. Scan parameters were equivalent to those in the original saccade experiments except that the interslice gap of 0.5 mm was used in monkeys to cover ventrally located visual areas. In monkeys, data from 138 runs with the two subjects were analyzed with the fixed-effect model. In humans, data from ten runs were averaged for each subject and analyzed with the random-effect model. BOLD signal changes under the control condition were measured at the voxel with the maximal  $t$  value within a spherical ROI (1 mm radius for monkeys; 3 mm radius for humans) around each homotopic peak defined in the saccade experiments. The signal changes were aver-

aged across left and right hemispheres in each ROI, and then statistically analyzed under the saccade and control conditions using two-way ANOVA (REGION  $\times$  CONDITION) using SAS/STAT software. We also performed the same statistical analysis using normalized signal changes. In monkeys, the signal changes in the frontal, parietal, parietooccipital, and temporal ROIs were normalized with those in the ROI of V3/V3A, since it was the only occipital homotopic region included in the brain volume scanned in the original saccade experiments. In humans, the signal changes in the ROIs other than the occipital ones were normalized with those averaged in all the occipital ROIs.

#### Acknowledgments

We thank S. Konishi, T. Asari, K. Homma, and T. Watanabe for technical collaboration and discussion. This work was funded by a Grant-in-Aid for Scientific Research (C) (11680803) to I.H.; and a Grant-in-Aid for Specially Promoted Research (14002005) to Y.M. from Ministry of Education, Culture, Sports, Science and Technology of Japan. M.K. was supported by Research Fellowships of the Japan Society for the Promotion of Science for Young Scientists (11804).

Received: July 7, 2003

Revised: December 2, 2003

Accepted: January 20, 2004

Published: March 3, 2004

#### References

- Andersen, R.A., Asanuma, C., Essick, G., and Siegel, R.M. (1990). Corticocortical connections of anatomically and physiologically defined subdivisions within the inferior parietal lobule. *J. Comp. Neurol.* 296, 65–113.
- Andersen, R.A., Snyder, L.H., Bradley, D.C., and Xing, J. (1997). Multimodal representation of space in the posterior parietal cortex and its use in planning movements. *Annu. Rev. Neurosci.* 20, 303–330.
- Astafiev, S.V., Shulman, G.L., Stanley, C.M., Snyder, A.Z., Van Essen, D.C., and Corbetta, M. (2003). Functional organization of human intraparietal and frontal cortex for attending, looking, and pointing. *J. Neurosci.* 23, 4689–4699.
- Beauchamp, M.S., Petit, L., Ellmore, T.M., Ingelholm, J., and Haxby, J.V. (2001). A parametric fMRI study of overt and covert shifts of visuospatial attention. *Neuroimage* 14, 310–321.
- Bremmer, F., Schlack, A., Shah, N.J., Zafiris, O., Kubischik, M., Hoffmann, K., Zilles, K., and Fink, G.R. (2001). Polymodal motion processing in posterior parietal and premotor cortex: a human fMRI study strongly implies equivalencies between humans and monkeys. *Neuron* 29, 287–296.
- Brewer, A.A., Press, W.A., Logothetis, N.K., and Wandell, B.A. (2002). Visual areas in macaque cortex measured using functional magnetic resonance imaging. *J. Neurosci.* 22, 10416–10426.
- Brodmann, K. (1905). Beitrage zur histologischen Lokalisation der Grosshirnrinde. III. Mitteilung. Die Rindenfelder der niederen Affen. *J. Psychol. Neurol.* 4, 177–226.
- Brodmann, K. (1909). Vergleichende Lokalisationslehre der Grosshirnrinde in ihren Prinzipien dargestellt auf Grund des Zellenbaues (Leipzig: Barth).
- Bruce, C.J., and Goldberg, M.E. (1985). Primate frontal eye fields. I. Single neurons discharging before saccades. *J. Neurophysiol.* 53, 603–635.
- Bruce, C.J., Goldberg, M.E., Bushnell, M.C., and Stanton, G.B. (1985). Primate frontal eye fields. II. Physiological and anatomical correlates of electrically evoked eye movements. *J. Neurophysiol.* 54, 714–734.
- Burgund, E.D., Lugar, H.M., Miezin, F.M., and Petersen, S.E. (2003). Sustained and transient activity during an object-naming task: a mixed blocked and event-related fMRI study. *Neuroimage* 19, 29–41.
- Chen, L.L., and Wise, S.P. (1995). Neuronal activity in the supplementary eye field during acquisition of conditional oculomotor associations. *J. Neurophysiol.* 73, 1101–1121.
- Colby, C.L., and Goldberg, M.E. (1999). Space and attention in parietal cortex. *Annu. Rev. Neurosci.* 22, 319–349.
- Colby, C.L., Duhamel, J.R., and Goldberg, M.E. (1993). Ventral intraparietal area of the macaque: anatomic location and visual response properties. *J. Neurophysiol.* 69, 902–914.
- Corbetta, M., Miezin, F.M., Shulman, G.L., and Petersen, S.E. (1993). A PET study of visuospatial attention. *J. Neurosci.* 13, 1202–1226.
- Corbetta, M., Akbudak, E., Conturo, T.E., Snyder, A.Z., Ollinger, J.M., Drury, H.A., Linenweber, M.R., Petersen, S.E., Raichle, M.E., Van Essen, D.C., and Shulman, G.L. (1998). A common network of functional areas for attention and eye movements. *Neuron* 21, 761–773.
- Corbetta, M., Kincade, J.M., Ollinger, J.M., McAvoy, M.P., and Shulman, G.L. (2000). Voluntary orienting is dissociated from target detection in human posterior parietal cortex. *Nat. Neurosci.* 3, 292–297.
- Courtney, S.M., Petit, L., Maisog, J.M., Ungerleider, L.G., and Haxby, J.V. (1998). An area specialized for spatial working memory in human frontal cortex. *Science* 279, 1347–1351.
- Driver, J., and Mattingley, J.B. (1998). Parietal neglect and visual awareness. *Nat. Neurosci.* 1, 17–22.
- Dubowitz, D.J., Chen, D.Y., Atkinson, D.J., Grieve, K.L., Gillikin, B., Bradley, W.G., Jr., and Andersen, R.A. (1998). Functional magnetic resonance imaging in macaque cortex. *Neuroreport* 9, 2213–2218.
- Fujii, N., Mushiaki, H., and Tanji, J. (1998). An oculomotor representation area within the ventral premotor cortex. *Proc. Natl. Acad. Sci. USA* 95, 12034–12037.
- Gattass, R., Gross, C.G., and Sandell, J.H. (1981). Visual topography of V2 in the macaque. *J. Comp. Neurol.* 201, 519–539.
- Genovese, C.R., Lazar, N.A., and Nichols, T. (2002). Thresholding of statistical maps in functional neuroimaging using the false discovery rate. *Neuroimage* 15, 870–878.
- Gitelman, D.R., Parrish, T.B., Friston, K.J., and Mesulam, M.M. (2002). Functional anatomy of visual search: regional segregations within the frontal eye fields and effective connectivity of the superior colliculus. *Neuroimage* 15, 970–982.
- Grosbras, M.H., Lobel, E., Van de Moortele, P.F., LeBihan, D., and Berthoz, A. (1999). An anatomical landmark for the supplementary eye fields in human revealed with functional magnetic resonance imaging. *Cereb. Cortex* 9, 705–711.
- Hasegawa, I., Fukushima, T., Ihara, T., and Miyashita, Y. (1998). Callosal window between prefrontal cortices: cognitive interaction to retrieve long-term memory. *Science* 281, 814–818.
- Hayashi, T., Konishi, S., Hasegawa, I., and Miyashita, Y. (1999). Mapping of somatosensory cortices with functional magnetic resonance imaging in anaesthetized macaque monkeys. *Eur. J. Neurosci.* 11, 4451–4456.
- Josephs, O., and Henson, R.N. (1999). Event-related functional magnetic resonance imaging: modelling, inference and optimization. *Philos. Trans. R. Soc. Lond. B Biol. Sci.* 354, 1215–1228.
- Kikyo, H., Ohki, K., and Miyashita, Y. (2002). Neural correlates for feeling-of-knowing: an fMRI parametric analysis. *Neuron* 36, 177–186.
- Konishi, S., Nakajima, K., Uchida, I., Kameyama, M., Nakahara, K., Sekihara, K., and Miyashita, Y. (1998). Transient activation of inferior prefrontal cortex during cognitive set shifting. *Nat. Neurosci.* 1, 80–84.
- Kwong, K.K., Belliveau, J.W., Chesler, D.A., Goldberg, I.E., Weisskoff, R.M., Poncelet, B.P., Kennedy, D.N., Hoppel, B.E., Cohen, M.S., Turner, R., et al. (1992). Dynamic magnetic resonance imaging of human brain activity during primary sensory stimulation. *Proc. Natl. Acad. Sci. USA* 89, 5675–5679.
- Lewis, J.W., and Van Essen, D.C. (2000). Mapping of architectonic subdivisions in the macaque monkey, with emphasis on parieto-occipital cortex. *J. Comp. Neurol.* 428, 79–111.
- Liu, T.T., Frank, L.R., Wong, E.C., and Buxton, R.B. (2001). Detection power, estimation efficiency, and predictability in event-related fMRI. *Neuroimage* 13, 759–773.
- Logothetis, N.K., Guggenberger, H., Peled, S., and Pauls, J. (1999). Functional imaging of the monkey brain. *Nat. Neurosci.* 2, 555–562.

- Logothetis, N.K., Pauls, J., Augath, M., Trinath, T., and Oeltermann, A. (2001). Neurophysiological investigation of the basis of the fMRI signal. *Nature* 412, 150–157.
- Logothetis, N.K., Merkle, H., Augath, M., Trinath, T., and Ugurbil, K. (2002). Ultra high-resolution fMRI in monkeys with implanted RF coils. *Neuron* 35, 227–242.
- Luna, B., Thulborn, K.R., Strojwas, M.H., McCurtain, B.J., Berman, R.A., Genovese, C.R., and Sweeney, J.A. (1998). Dorsal cortical regions subserving visually guided saccades in humans: an fMRI study. *Cereb. Cortex* 8, 40–47.
- Menon, R.S., and Kim, S.G. (1999). Spatial and temporal limits in cognitive neuroimaging with fMRI. *Trends Cogn. Sci.* 3, 207–216.
- Merriam, E.P., Colby, C.L., Thulborn, K.R., Luna, B., Olson, C.R., and Sweeney, J.A. (2001). Stimulus-response incompatibility activates cortex proximate to three eye fields. *Neuroimage* 13, 794–800.
- Mesulam, M.M. (1999). Spatial attention and neglect: parietal, frontal and cingulate contributions to the mental representation and attentional targeting of salient extrapersonal events. *Philos. Trans. R. Soc. Lond. B Biol. Sci.* 354, 1325–1346.
- Nakahara, K., Hayashi, T., Konishi, S., and Miyashita, Y. (2002). Functional MRI of macaque monkeys performing a cognitive set-shifting task. *Science* 295, 1532–1536.
- Nakamura, K., Chung, H.H., Graziano, M.S., and Gross, C.G. (1999). Dynamic representation of eye position in the parieto-occipital sulcus. *J. Neurophysiol.* 81, 2374–2385.
- Ogawa, S., Lee, T.M., Kay, A.R., and Tank, D.W. (1990). Brain magnetic resonance imaging with contrast dependent on blood oxygenation. *Proc. Natl. Acad. Sci. USA* 87, 9868–9872.
- Ohbayashi, M., Ohki, K., and Miyashita, Y. (2003). Conversion of working memory to motor sequence in the monkey premotor cortex. *Science* 301, 233–236.
- Paus, T. (1996). Location and function of the human frontal eye-field: a selective review. *Neuropsychologia* 34, 475–483.
- Perry, R.J., and Zeki, S. (2000). The neurology of saccades and covert shifts in spatial attention: an event-related fMRI study. *Brain* 123, 2273–2288.
- Petit, L., and Haxby, J.V. (1999). Functional anatomy of pursuit eye movements in humans as revealed by fMRI. *J. Neurophysiol.* 82, 463–471.
- Petit, L., Clark, V.P., Ingeholm, J., and Haxby, J.V. (1997). Dissociation of saccade-related and pursuit-related activation in human frontal eye fields as revealed by fMRI. *J. Neurophysiol.* 77, 3386–3390.
- Petrides, M., and Pandya, D.N. (1994). Comparative architectonic analysis of the human and the macaque frontal cortex. In *Handbook of Neuropsychology*, F. Boller and J. Grafman, eds. (Amsterdam: Elsevier), pp. 17–58.
- Picard, N., and Strick, P.L. (2001). Imaging the premotor areas. *Curr. Opin. Neurobiol.* 11, 663–672.
- Preuss, T.M., Stepniewska, I., and Kaas, J.H. (1996). Movement representation in the dorsal and ventral premotor areas of owl monkeys: a microstimulation study. *J. Comp. Neurol.* 371, 649–676.
- Rorden, C., and Brett, M. (2000). Stereotaxic display of brain lesions. *Behav. Neurol.* 12, 191–200.
- Rosano, C., Sweeney, J.A., Melchitzky, D.S., and Lewis, D.A. (2003). The human precentral sulcus: chemoarchitecture of a region corresponding to the frontal eye fields. *Brain Res.* 972, 16–30.
- Sakai, K., Hikosaka, O., Miyauchi, S., Takino, R., Sasaki, Y., and Putz, B. (1998). Transition of brain activation from frontal to parietal areas in visuomotor sequence learning. *J. Neurosci.* 18, 1827–1840.
- Schall, J.D. (1997). Visuomotor areas of the frontal lobe. In *Cerebral Cortex*, K.S. Rockland, J.H. Kaas, and A. Peters, eds. (New York: Plenum Publishers), pp. 527–638.
- Schlag, J., and Schlag-Rey, M. (1987). Evidence for a supplementary eye field. *J. Neurophysiol.* 57, 179–200.
- Schmitt, F., Stehling, M.K., and Turner, R. (1998). *Echo-Planar Imaging: Theory, Technique and Application* (Berlin: Springer Verlag).
- Seltzer, B., and Pandya, D.N. (1980). Converging visual and somatic sensory cortical input to the intraparietal sulcus of the rhesus monkey. *Brain Res.* 192, 339–351.
- Seltzer, B., and Pandya, D.N. (1986). Posterior parietal projections to the intraparietal sulcus of the rhesus monkey. *Exp. Brain Res.* 62, 459–469.
- Sereno, M.I., Pitzalis, S., and Martinez, A. (2001). Mapping of contralateral space in retinotopic coordinates by a parietal cortical area in humans. *Science* 294, 1350–1354.
- Snedecor, G.W., and Cochran, W.G. (1989). *Statistical Methods*, Eighth Edition (Ames, Iowa: Iowa State University Press).
- Snyder, L.H., Batista, A.P., and Andersen, R.A. (2000). Saccade-related activity in the parietal reach region. *J. Neurophysiol.* 83, 1099–1102.
- Sommer, M.A., and Wurtz, R.H. (2002). A pathway in primate brain for internal monitoring of movements. *Science* 296, 1480–1482.
- Stefanacci, L., Reber, P., Costanza, J., Wong, E., Buxton, R., Zola, S., Squire, L., and Albright, T. (1998). fMRI of monkey visual cortex. *Neuron* 20, 1051–1057.
- Suzuki, H., and Azuma, M. (1983). Topographic studies on visual neurons in the dorsolateral prefrontal cortex of the monkey. *Exp. Brain Res.* 53, 47–58.
- Sweeney, J.A., Mintun, M.A., Kwee, S., Wiseman, M.B., Brown, D.L., Rosenberg, D.R., and Carl, J.R. (1996). Positron emission tomography study of voluntary saccadic eye movements and spatial working memory. *J. Neurophysiol.* 75, 454–468.
- Talairach, J., and Tournoux, P. (1988). *Co-planar Stereotaxic Atlas of the Human Brain*. (New York: Thieme Medical Publishers).
- Tehovnik, E.J., Sommer, M.A., Chou, I.H., Slocum, W.M., and Schiller, P.H. (2000). Eye fields in the frontal lobes of primates. *Brain Res. Brain Res. Rev.* 32, 413–448.
- Tomita, H., Ohbayashi, M., Nakahara, K., Hasegawa, I., and Miyashita, Y. (1999). Top-down signal from prefrontal cortex in executive control of memory retrieval. *Nature* 401, 699–703.
- Tootell, R.B., and Hadjikhani, N. (2001). Where is 'dorsal V4' in human visual cortex? Retinotopic, topographic and functional evidence. *Cereb. Cortex* 11, 298–311.
- Tsao, D.Y., Freiwald, W.A., Knutsen, T.A., Mandeville, J.B., and Tootell, R.B. (2003a). Faces and objects in macaque cerebral cortex. *Nat. Neurosci.* 6, 989–995.
- Tsao, D.Y., Vanduffel, W., Sasaki, Y., Fize, D., Knutsen, T.A., Mandeville, J.B., Wald, L.L., Dale, A.M., Rosen, B.R., Van Essen, D.C., et al. (2003b). Stereopsis activates V3A and caudal intraparietal areas in macaques and humans. *Neuron* 39, 555–568.
- Vanduffel, W., Fize, D., Mandeville, J.B., Nelissen, K., Van Hecke, P., Rosen, B.R., Tootell, R.B., and Orban, G.A. (2001). Visual motion processing investigated using contrast agent-enhanced fMRI in awake behaving monkeys. *Neuron* 32, 565–577.
- Vanduffel, W., Fize, D., Peuskens, H., Denys, K., Sanaert, S., Todd, J.T., and Orban, G.A. (2002). Extracting 3D from motion: differences in human and monkey intraparietal cortex. *Science* 298, 413–415.
- Van Essen, D.C., Lewis, J.W., Drury, H.A., Hadjikhani, N., Tootell, R.B., Bakircioglu, M., and Miller, M.I. (2001). Mapping visual cortex in monkeys and humans using surface-based atlases. *Vision Res.* 41, 1359–1378.
- Von Bonin, G., and Bailey, P. (1947). *The Neocortex of Macaca Mulatta* (Urbana, IL: University of Illinois Press).
- Wise, S.P., Boussaoud, D., Johnson, P.B., and Caminiti, R. (1997). Premotor and parietal cortex: corticocortical connectivity and combinatorial computations. *Annu. Rev. Neurosci.* 20, 25–42.
- Zeki, S.M. (1977). Simultaneous anatomical demonstration of the representation of the vertical and horizontal meridians in areas V2 and V3 of rhesus monkey visual cortex. *Proc. R. Soc. Lond. B Biol. Sci.* 195, 517–523.